Vapor thermodynamics and fluid merit for pulsating heat pipe

Vadim S. Nikolayev[1], Iaroslav Nekrashevych

Service de Physique de l'Etat Condensé, CEA, CNRS, Université Paris-Saclay, CEA Saclay, 91191 Gif-sur-Yvette Cedex, France

Abstract

In this communication, we discuss a theoretical description of the vapor phase thermodynamics in the pulsating heat pipe (PHP), to be used in the numerical simulations. We advance a theory based on simulation results that allows us to derive a theoretical expression for a dimensionless quantity showing elastic properties of the vapor for a given fluid. One can use this quantity to evaluate the fluid merit for use in the PHP. This theory is confronted to the simulation results obtained with the PHP simulation code CASCO. We compare the merit of water, ethanol, and FC-72 and show that water possesses better properties for use in PHP.

Keywords: Pulsating heat pipe, Oscillation, Merit number, Numerical simulation

1. INTRODUCTION

The pulsating (or oscillating) heat pipe (PHP) is a simple capillary tube bent into branches meandering between hot and cold spots and partially filled with a two-phase, usually single component, working fluid. During PHP functioning, a moving pattern of multiple vapor bubbles separated by liquid plugs forms spontaneously inside the tube. Because of their simplicity and high performance, PHP's are often considered as highly promising. During the last decade, researchers have extensively studied PHP [1, 2]. However their functioning is not completely understood. Tools for their dimensioning are still absent. Perhaps the most critical issue for the PHP modeling is the vapor phase thermodynamic state. Because of the nonstationary functioning of PHP, the vapor state varies, so both the current state and its change should be understood. The vapor at equilibrium with the liquid (at saturation) condenses at compression without giving an elastic response necessary for the oscillations. An important question concerns the conditions at which the elastic response exists and its out-of-equilibrium theoretical modeling. In the PHP modeling, the state of a vapor bubble situating inside the PHP tube is often described by the single temperature T_v. Such a description is precise during the fast bubble motion, where the thickness of the thermal boundary layer developed inside the vapor is much smaller than the tube diameter due to the weakness of the vapor thermal conductivity. In other cases, T_v corresponds to some spatially averaged temperature.

In the existing PHP modeling, two approaches can be distinguished. In their pioneering article on the PHP modeling, Shafii et al. [3] assumed that the vapor behavior may be assimilated to that of the ideal gas that is described by the equation of state (EOS)

$$p = mR_{\rm v}T_v/V, \tag{1}$$

with m, the vapor mass, p, its pressure, V, its volume, and $R_{\rm v}$, the vapor gas constant. Such an assumption was adopted in a large majority of the modeling approaches.

Instead of using EOS (1), d'Entremont and Thome [4], Aubin et al. [5] assumed the vapor to always remain at saturation evolving along the gas branch of coexistence curve (right part of the red curve in Fig. 1b), where

$$p = p_{sat}(T_v). \tag{2}$$

During the volume variation (vapor compression/dilatation) due to oscillations, vapor density ρ_{sat} changes. They find the new vapor temperature by inverting the $\rho_{sat}(T)$ curve (see Fig. 2 below). We note that the saturated vapor model can also create a kind of elastic response: when the vapor volume reduces at constant mass, $\rho_{\rm sat}$ increases (i.e. $\rho_{\rm sat}^{-1}$ decreases) and the pressure rises according to Fig. 1b together with the vapor temperature. Note that the such an assumption is hardly justified because it is not clear why the fluid cannot deviate from this particular trajectory (i.e., the coexistence curve) in the thermodynamic space. In addition, a change in vapor enthalpy appearing when the vapor evolves along the coexistence curve is not balanced; the energy conservation is not satisfied.

Many modeling approaches [6–11] try to reconcile two these models. On one hand, Eq. (1) is applied to describe the vapor state. On the other, the tube wall-fluid heat exchange rate is assumed to be proportional to the difference $(T_w - T_v)$ of tube wall and

[1]Corresponding author: vadim.nikolayev@cea.fr, Ph.: +33169089488

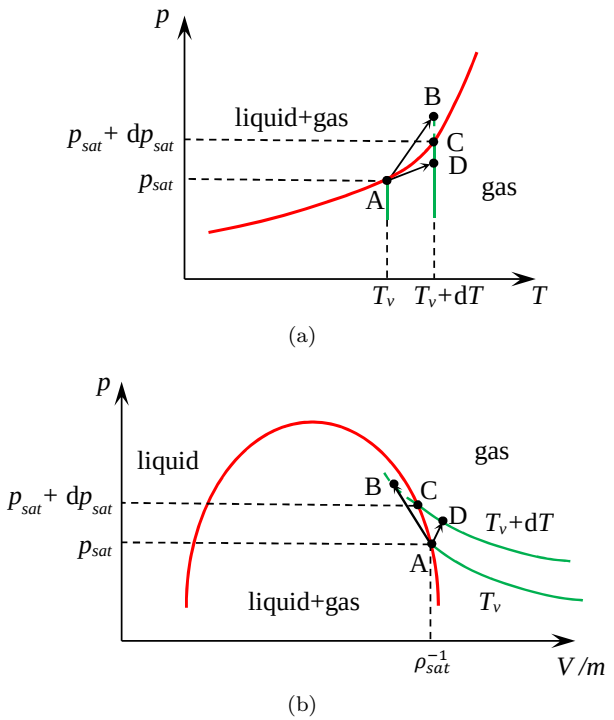

Fig. 1: Fluid phase diagram (a) in the $p-T$ coordinates and (b) in the $p-V$ coordinates. Gas is called also superheated vapor. The isotherms are shown in green and the coexistence curve in red. The same states A, B, C, D are shown in both figures.

vapor temperatures. This expression is usually justified by the hypothesis that the vapor is saturated ($T_v = T_{\rm sat}$). The wall heat flux is spent mainly for the film evaporation/condensation, the rate of which is well known to be proportional to $(T_{\rm w} - T_{\rm sat})$.

The assumptions of superheated vapor and saturated vapor are however mutually exclusive if applied in dynamics. Indeed, the pressure of saturated vapor is entirely defined by T_v (cf. Eq. 2) rather than by T_v, m, and V (cf. Eq. 1). In this communication we suggest a modeling approach in which the vapor is allowed to change its state from superheated to saturated. In the second part of this communication we discuss the fluid merit number that appears to be linked to the vapor thermodynamic state evolution in PHPs.

2. VAPOR THERMODYNAMIC STATE IN STATICS

The phase diagram for common fluids at equilibrium is sketched in Figs. 1. The fluid equation of state (EOS, i.e. the set of thermodynamic states that can be occupied by the fluid) is a surface in the coordinates (p, V, T). The two phase (liquid-gas) coexistence region situates inside the red bell-shaped curve called coexistence curve as seen in the projection of this surface to the $p-V$ plane (Fig. 1b). Its projection

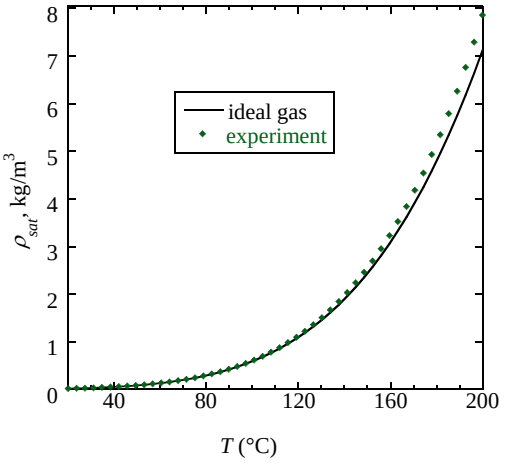

Fig. 2: Saturated vapor density (that corresponding to the boundary between the regions "gas" and "liquid+gas" in Fig. 1b) for water. The line corresponds to Eq. (3), while the characters are experimental data.

to the $p-T$ plane is just a line called saturation curve shown in Fig. 1a. A part below the saturation curve corresponds to the gas phase (in which point D is situated), a part above, to the liquid. The point A (saturated vapor) situates at the coexistence curve. The gas state (D) is often referred to as superheated vapor because, at equal pressures, its temperature is higher than that of the saturated vapor, $T_D > T_{sat}(p_D)$, cf. Fig. 1a.

The above assumption about the vapor behavior similar to the ideal gas can be easily checked by comparing the density ρ_{sat} of saturated vapor calculated from Eqs. (1-2)

$$\rho_{sat} = \frac{p_{sat}(T_v)}{R_v T_v}. \qquad (3)$$

to the experimental data (Fig. 2). One can see that the water vapor can be approximated with good accuracy by the ideal gas. For this reason, there is no need to use more sophisticated EOS forms.

When the superheated vapor is compressed or dilated (i.e. its volume changes), the vapor state follows EOS (1) and the pressure responds, which creates a restoring force for the oscillation. Such a model has been confirmed experimentally. Gully et al. [12] have shown that the vapor superheating (with respect to $T_{sat}(p)$) can be of the order of 10K. The same team has shown that the vapor is nearly always superheated so it rarely approaches the coexistence curve. However, to manage such events in the model, a solution proposed by Shafii et al. [3] can be used. The vapor state obeys Eq. (1) as long as $p < p_{sat}(T_v)$ (point D in Figs. 1). Once the pressure obtained with Eq. (1) becomes larger than $p_{sat}(T_v)$, the vapor pressure is imposed to be equal to p_{sat} and the vapor mass is made to be equal to $\rho_{sat} V$; the extra vapor mass is added to the liquid plug for mass conserva-

tion. In other words, the point B in Figs. 1 is shifted to the point C.

The vapor temperature is not entirely homogeneous during vapor compression or expansion. Thermal boundary layers are developed near both the tube walls at temperature T_w and the liquid films at temperature T_{sat} covering the walls. The thickness of these layers is a complex yet unsolved issue. Direct numerical simulations [12] of the gas flow during oscillatory compression performed with ANSYS CFX software for oxygen at about 70K showed a thickness of ~ 0.25 mm in the tube of 2 mm diameter. The vapor flow remains mostly laminar in the thermal boundary layers; turbulent mixing is absent near the wall. For this reason, in one-dimensional models one can reasonably assume that the vapor bulk can be described by a unique temperature. Because of a large temperature difference, the vapor heat exchange is mainly that with the dry wall area of the length L_d. The heat exchange coefficient is $U_v = Nu_v\lambda_v/d$ and the heat exchange rate is

$$\dot{Q}_v = U_v \pi d L_d (T_w - T_v). \tag{4}$$

The above numerical calculation resulted in $Nu_v \simeq 6$. In the multi-branch PHPs , the heat exchange with the wetted wall area is usually smaller because of the small temperature difference $(T_{sat} - T_v)$ and is neglected here.

3. VAPOR STATE CHANGE

The vapor energy equation is different for superheated vapor different thermodynamic state and should be derived from the first law of thermodynamics.

3.1. Gas state change

When the vapor is superheated and obeys the ideal gas law (1), Shafii et al. [3] showed that it can be described by the equation (see [13] for its detailed derivation)

$$mc_{vv}\dot{T}_v = R_v T_v \dot{m} - p\dot{V} + \dot{Q}_v \tag{5}$$

where dot means the time derivative. This equation can be reduced by using both EOS (1) and Mayer's relation $c_{pv} = c_{vv} + R_v$ valid for the ideal gas:

$$\dot{p} = \frac{p}{T_v}\frac{\gamma}{\gamma - 1}\dot{T}_v - \frac{\dot{Q}_v}{V}, \tag{6}$$

where $\gamma = c_{pv}/c_{vv}$ is the adiabatic index.

If one assumes that the vapor *always* satisfies the vapor domain EOS (1) and *never* reaches the saturation state, the numerical simulation code becomes unstable at large heat powers or large simulation times via T_v increasingly large temporal oscillation around more stable T_w. A T_v rise causes a p rise through EOS (1), which leads to T_{sat} increase. The vapor mass change rate is defined by the expression

$$\dot{m} \sim (T_w - T_{sat}) \tag{7}$$

as explained above and can thus become negative. Because of eq. (5) where $\dot{m}$ is the largest term, T_v decreases. However its decrease is much stronger than its previous increase. This effect causes oscillations that lead to huge vapor temperature (either positive or negative) and eventually the code crash. To prevent it, the saturation vapor state needs to be introduced.

3.2. Saturated vapor state change

When the vapor is at saturation, it obeys the law (2). One may assume that the saturation is attained in the condenser where there are no dry film wall; the vapor sensible heat exchange $\dot{Q}_v$ with the environment is negligibly small so

$$\dot{T}_v = 0, \tag{8}$$

and the vapor pressure does not change either. Phase change at the vapor-liquid interfaces occurs to maintain a constant vapor density ρ_{sat} and the vapor mass evolution obeys

$$\dot{m} = \dot{m}_{sat} \equiv \rho_{sat}\dot{V}. \tag{9}$$

instead of Eq. (7). In other words, the vapor condenses when compressed and vice-versa, evaporation occurs when the vapor is dilated. The condensed (or evaporated) liquid mass should be added to (or removed from) the liquid plug to conserve the total fluid mass.

The $\dot{m}$ definition (9) cannot *always* be applied. Indeed, this would lead to impossibility for a bubble to leave the saturation state even for a strong film condensation (i.e. vapor mass reduction) or the bubble expansion. Within an adequate thermodynamic model, both these changes should lead to the pressure reduction so that the vapor may become again superheated, cf. Fig. 1b). For this reason, an additional criterion based on the pressure change needs to be used as described hereafter.

Suppose the vapor is at saturation curve (point A in Figs. 1). While the vapor remains to be saturated, its evolution is governed by Eqs. (8,9), which means that the vapor state does not move from the point A. To determine if the vapor should exit it, one needs to calculate the pressure change $\mathrm{d}p_{gas} = \dot{p}\mathrm{d}t$ under the hypothesis that the vapor is superheated, where $\mathrm{d}t$ is the time step and $\dot{p}$ is obtained from the EOS (with Eq. (6) for the ideal gas EOS). Since the point A situates at the coexistence curve, all the parameters in Eq. (6) have to be taken at the coexistence. In Figs. 1, the pressure change $\mathrm{d}p_{gas}$ corresponds to the transitions A→B or A→D. The corresponding T_v change is $\mathrm{d}T = \dot{T}_v\mathrm{d}t$ with $\dot{T}_v$ given by Eq. (5).

Two situations are possible. In the first case, the new vapor state would fall inside the coexistence curve (point B in Figs. 1). Evidently, in this case the vapor should remain to be saturated. In the second case (point D in Figs. 1), the vapor should quit the saturation state and become gas; the mass and temperature derivatives should now be defined with Eqs. (5, 7). Since the isotherm is a decreasing function (see Figs. 1), to distinguish two these cases, one needs to compare $\mathrm{d}p_{gas}$ with the change

$$\mathrm{d}p_{sat} = \left.\frac{\mathrm{d}p}{\mathrm{d}T}\right|_{sat} \mathrm{d}T, \tag{10}$$

that correspond to the transition A→C in Figs. 1. The vapor stays at saturation while $\mathrm{d}p_{gas} \geq \mathrm{d}p_{sat}$. The vapor leaves the saturation state when $\mathrm{d}p_{gas} < \mathrm{d}p_{sat}$. Note that Figs. 1 apply to the case $\mathrm{d}T > 0$. One can easily check that the same criterion is valid for the case $\mathrm{d}T < 0$.

4. VAPOR COMPRESSION MERIT NUMBER

The above vapor state change criterion (i.e. a criterion of exiting the saturation state) reduces to

$$\frac{1}{N} - \frac{\dot{Q}_v}{\dot{T}_v V} \left.\frac{\mathrm{d}T}{\mathrm{d}p}\right|_{sat} < 1, \tag{11}$$

where

$$N = \frac{(\gamma-1)T}{\gamma p_{sat}(T)} \left.\frac{\mathrm{d}p}{\mathrm{d}T}\right|_{sat}. \tag{12}$$

For a given fluid, the number N depends only on the temperature (Fig. 3) and exhibits a weak temperature variation. For some fluids like FC-72, $N < 1$, while for others (ethanol or water), $N > 1$ over all the temperature range of interest.

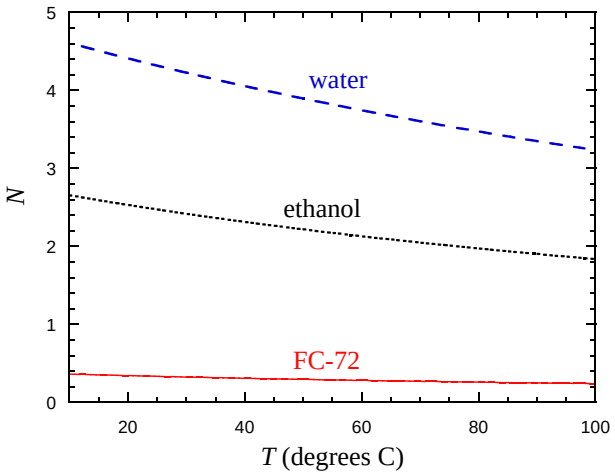

Fig. 3: Fluid merit number N related to the vapor compression.

The objective is to analyze the fluid merit for the PHP startup and stable functioning. This analysis is based on the PHP simulation results obtained with the numerical code CASCO [14] showing the importance of the bubble nucleation and growth in the evaporator section. In particular, the stable oscillations start when multiple vapor bubbles are generated in the evaporator. Consider a bubble freshly generated at a nucleation (hot) spot. A second bubble can be generated at the same hot spot while the first bubble is advected because of the liquid plug displacement during oscillating motion. Two bubbles become neighbors. The oscillations are amplified when both bubbles expand so a large pressure difference is created. However, when the growth of the second bubble leads to retraction and disappearance of the first, the oscillating motion is weak and the PHP performance is poor. However the growth of the second bubble leads inevitably to the compression of the first. At its birth, the vapor in the bubble is saturated. If the vapor remains saturated in the first bubble after generation of the second, the growth of the second bubble will lead to the contraction (because of condensation) of the first and its eventual disappearance. If, on the contrary, the vapor in the first bubble becomes superheated (i.e. elastic) it can resit to the compression and expand if evaporation into it occurs. For this reason, the ability of the vapor state change (saturated→superheated) is the major factor for the sustainment of oscillations.

To analyze the vapor state change criterion (11), the first (N^{-1}) term is more important than the second containing $\dot{Q}_v$. The mean value of the latter is generally small (because of the weak vapor heat exchange) and positive: the tube walls are hotter than vapor in the evaporator section. One can see that if $N < 1$, the bubbles can rarely exit the saturation state. The only effect that can drive them out of saturation is the vapor heat exchange. On the contrary, the bubbles of the fluids with $N > 1$ quit easier the saturation state helping to establish the stable oscillations. For this reason, N characterizes the fluid merit for usage in PHPs.

Such a fluid merit definition is coherent with the oscillation start-up threshold found analytically for the single-branch PHP [2, 15]. It was found that the oscillation start-up threshold decreases (which is beneficial) with $\mathrm{d}p/\mathrm{d}T|_{sat}$.

The number N characterizes a capacity of the given fluid to provide oscillatory behavior. However, it is evident that the fluid merit is not defined solely by N. The liquid phase properties are also important. A "good" fluid should have a small viscosity (for small viscous dissipation). High values of latent heat and heat capacity of liquid are required to provide an efficient heat exchange.

5. SIMULATION RESULTS

The simulation is performed with in-house CASCO software (French abbreviation for Code Avancé de Simulation du Caloduc Oscillant: advanced PHP simulation code [14, 16] for three different fluids (water, ethanol and FC-72) for the flat PHP geometry shown in Fig. 4. The total power P_e injected into

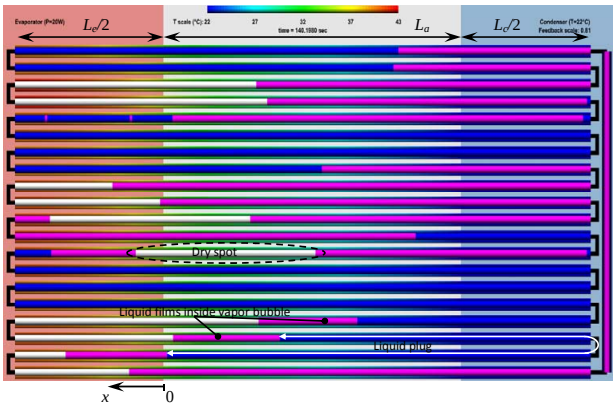

Fig. 4: The PHP geometry pictured by the PHP_Viewer postprocessor of the CASCO software. Thin liquid films (in violet) cover the internal tube walls inside of the vapor bubbles, except of the dry spot areas (white). The liquid plugs are shown in blue. The wall temperature is shown with the color varying from blue to red; its scale is indicated at the top. The round turns are not pictured for simplicity; black lines just connect equivalent points which correspond to the extreme points of each turn.

the evaporator and the temperature T_c at the internal tube walls are imposed in the simulation. Some portions of tube belong to the evaporator. The length of one portion is denoted L_e and their number is referred to as N_{turn}. To study the local fluid-tube thermal interaction, each of them is assumed to be heated independently and homogeneously, with the power P_e/N_{turn}. The PHP parameters are shown in Table 1.

The liquid film thickness δ is a fixed parameter in CASCO. It is calculated a posteriori from the average menisci velocity observed in simulations by using the Aussillous and Quéré formula [17, 18]. The thickness is not very sensitive to the velocity and can be fixed for each fluid. In present simulations, it is 40μm for water, 80μm for ethanol and 60μm for FC-72. The performance of water and ethanol can be illustrated by Fig. 5. One can see that in this particular situation both water and ethanol PHP show stable chaotic oscillations after an initial start-up period. In agreement with the above theory, the start-up of ethanol PHP in horizontal orientation is more difficult than of water PHP. In particular, an initial evaporator overheating above the stable functioning temperature is needed to start-up the oscillations. In the beginning

Table 1: Parameters used for the simulation.

Length of evaporator	$L_e = 126$ mm
Length of adiabatic section	$L_a = 126$ mm
Length of condenser	$L_c = 110$ mm
Number of turns	$N_{turn} = 10$
Feedback section length	$L_{fb} = 130$ mm
Filling ratio	$\phi = 0.5$
Inner diameter	$d = 1.4$ mm
Outer diameter	3.2 mm
Condenser temperature	$T_c = 22°$C
Tube material	Copper
Time step	0.01 ms
Tube mesh size	2 mm
Bubble deletion threshold	$L_{thr} = 10$ μm
Nucleated bubble length	$L_{nucl} = 500$ μm
Nucleation barrier	$\Delta T_{nucl} = 15°$C

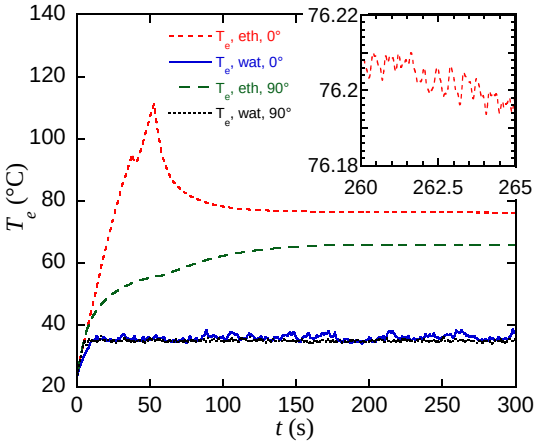

Fig. 5: Time evolution of the averaged over evaporator tube sections temperature T_e for water and ethanol in horizontal (0°) and vertical favorable (90°, evaporator under condenser) orientations for P_e = 100 W.

of evolution, most bubbles that existed initially disappear (the liquid plugs coalesce) when their length becomes smaller than L_{thr}. The system starts up by generation of multiple bubbles as discussed in detail in our previous paper [14].

Another manifestation of the difference between these fluids concerns different orientations. One can see that for water the performances in horizontal and vertical orientations are similar. It means that the pressure difference in the neighboring bubbles created during oscillation is much larger than the hydrostatic pressure (which is beneficial). This is not the case for ethanol, where the difference between horizontal and vertical orientations is striking.

The case of FC-72 is very different: for the horizontal orientation, stable oscillations appear only for a few particular choices of parameters. Usually the system dries out without attaining a stable oscillation regime. The initial stage dynamics is different from

water or ethanol cases. After disappearance of the initial small bubbles and heating of the tube walls in evaporator section, bubble generation starts in long liquid plugs. At each time step, several bubbles of the size L_{nucl} are allowed to be nucleated sequentially once the difference between the wall temperature and the local saturation temperature exceeds the nucleation barrier [14]. As the vapor density is smaller, the host plug ends displace slightly during each nucleation event to accommodate the newly generated bubble volume. Therefore, each subsequent bubble nucleation leads to compression of the previously nucleated bubbles. Because of the small $N < 1$ for FC-72, in many cases, a new nucleation leads to recondensation of the bubbles that were nucleated at the previous time step bubble (Fig. 6). Instead of expanding in the water case [14], newly generated bubbles recondense. This process does not create oscillations so the PHP eventually dries out.

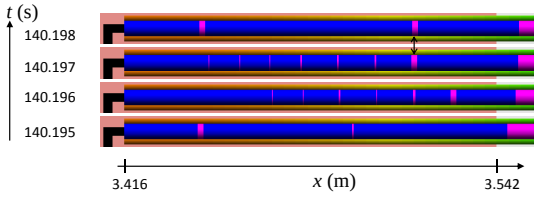

Fig. 6: Bubble generation and disappearance in the evaporator for the FC-72 case in horizontal orientation. For consecutive simulated time steps are shown. The temperature scale corresponds to Fig. 4, where the whole PHP is presented for $t = 140.198$ s. The evaporator part of the 16th from the bottom branch is shown here. Most newly nucleated bubbles disappear at the next time step. The only bubble that survives two time steps is shown with the arrow.

6. CONCLUSIONS

In conclusion, we derive here the fluid merit factor showing the vapor elastic properties in the PHP. One notes that this factor corresponds only to the vapor phase properties and not to the liquid properties responsible for many other phenomena impacting the fluid merit like liquid viscosity and wetting properties. Such a merit factor allows us to explain the numerical simulation results obtained for three different fluids. We show that FC-72 is generally worse for PHP applications than ethanol or water.

ACKNOWLEDGMENTS

The financial contribution of ESA in the framework of the MAP INWIP is acknowledged.

NOMENCLATURE

$\dot{Q}, P$	power (W)
c_{pv}	vapor specific heat at constant pressure (J/(kg·K))
c_{vv}	vapor specific heat at constant volume (J/(kg·K))
d	tube inner diameter (m)
h_{lv}	latent heat (J/kg)
L	length (m)
m	mass of vapor (kg)
N	fluid merit number
N_{turn}	number of PHP turns
Nu	Nusselt number
p	pressure (Pa)
R	gas constant (J/(kg·K))
S	cross-section area (m^2)
T	temperature (K)
t	time (s)
U	heat transfer coefficient (W/(m^2K))

Greek symbols

Δ	difference
δ	thickness (m)
γ	vapor adiabatic index
λ	heat conductivity (W/(m·K))
ϕ	volume fraction of liquid in PHP
ρ	density (kg/m^3)
V	vapor bubble volume (m^3)

Subscripts

a	adiabatic
c	condenser
d	dry
e	evaporator
f	liquid film
fb	feedback section (vertical in Fig. 4)
l	liquid
$nucl$	nucleation
sat	at saturation
thr	threshold
v	vapor
w	internal tube wall

REFERENCES

[1] M. Marengo, V. Nikolayev, Pulsating Heat Pipes: Experimental Analysis, Design and Applications, in: J. R. Thome (Ed.), Encyclopedia of Two-Phase Heat Transfer and Flow IV, vol. 1: Modeling of Two-Phase Flows and Heat Transfer, World Scientific, ISBN 978-981-3234-36-9, 1 – 62, URL http://www.worldscientific.com/worldscibooks/10.1142/10831, 2018.

[2] V. Nikolayev, M. Marengo, Pulsating Heat Pipes: Basics of Functioning and Numerical Modeling, in: J. R. Thome (Ed.), Encyclopedia of Two-Phase Heat Transfer and Flow IV, vol. 1: Modeling of Two-Phase Flows and Heat Transfer, World Scientific, ISBN 978-981-3234-36-9, 63 – 139, URL http://www.worldscientific.com/worldscibooks/10.1142/10831, 2018.

[3] M. B. Shafii, A. Faghri, Y. Zhang, Thermal Modeling of Unlooped and Looped Pulsating Heat Pipes, J. Heat Transfer 123 (6) (2001) 1159 – 1172, doi:10.1115/1.1409266.

[4] B. P. d'Entremont, J. R. Thome, A Numerical Study of Pulsating Heat Pipe Performance, in: Proc.InterPACKICNMM 2015, V003T10A025, doi:10.1115/ipack2015-48350, 2015.

[5] P. Aubin, B. P. d'Entremont, D. Sturzenegger, R. Haynau, J. R. Schaadt, J. R. Thome, 1D Mechanistic Model and Simulation Code for Closed-Loop Pulsating Heat Pipes, in: J. R. Thome (Ed.), Encyclopedia of Two-Phase Heat Transfer and Flow IV, vol. 1: Modeling of Two-Phase Flows and Heat Transfer, World Scientific, ISBN 978-981-3234-36-9, 141 – 208, URL http://www.worldscientific.com/worldscibooks/10.1142/10831, 2018.

[6] R. T. Dobson, Theoretical and experimental modelling of an open oscillatory heat pipe including gravity, Int. J. Therm. Sci. 43 (2) (2004) 113 – 119, doi:10.1016/j.ijthermalsci.2003.05.003.

[7] B. Holley, A. Faghri, Analysis of pulsating heat pipe with capillary wick and varying channel diameter, Int. J. Heat Mass Transfer 48 (13) (2005) 2635 – 2651, doi:10.1016/j.ijheatmasstransfer.2005.01.013.

[8] W. Shao, Y. Zhang, Effects of Film Evaporation and Condensation on Oscillatory Flow and Heat Transfer in an Oscillating Heat Pipe, J. Heat Transfer 133 (4) (2011) 042901, doi:10.1115/1.4002780.

[9] P. Cheng, H. Ma, A Mathematical Model of an Oscillating Heat Pipe, Heat Transfer Eng. 32 (11-12) (2011) 1037–1046, doi:10.1080/01457632.2011.556495.

[10] M. Mameli, M. Marengo, S. Zinna, Numerical model of a multi-turn Closed Loop Pulsating Heat Pipe: Effects of the local pressure losses due to meanderings, Int. J. Heat Mass Transfer 55 (4) (2012) 1036 – 1047, doi:10.1016/j.ijheatmasstransfer.2011.10.006.

[11] H. Ma, Oscillating Heat Pipes, Springer, New York, ISBN 978-1-4939-2504-9, doi:10.1007/978-1-4939-2504-9, 2015.

[12] P. Gully, F. Bonnet, V. Nikolayev, N. Luchier, T. Q. Tran, Evaluation of the vapor thermodynamic state in PHP, in: Proc. 17th Int. Heat Pipe Conf., Begell, ISBN 978-1-56700-453-3, 369 – 376, 2015.

[13] V. S. Nikolayev, Comment on "Flow and heat transfer of liquid plug and neighboring vapor slugs in a pulsating heat pipe" by Yuan, Qu, & Ma, Int. J. Heat Mass Transfer 54 (9-10) (2011) 2226 – 2227, doi:10.1016/j.ijheatmasstransfer.2011.01.007.

[14] I. Nekrashevych, V. S. Nikolayev, Effect of tube heat conduction on the pulsating heat pipe start-up, Appl. Therm. Eng. 117 (2017) 24 – 29, doi:10.1016/j.applthermaleng.2017.02.013.

[15] V. S. Nikolayev, Effect of tube heat conduction on the single branch pulsating heat pipe start-up, Int. J. Heat Mass Transfer 95 (2016) 477 – 487, doi:10.1016/j.ijheatmasstransfer.2015.12.016.

[16] V. S. Nikolayev, A Dynamic Film Model of the Pulsating Heat Pipe, J. Heat Transfer 133 (8) (2011) 081504, doi:10.1115/1.4003759.

[17] P. Aussillous, D. Quéré, Quick deposition of a fluid on the wall of a tube, Phys. Fluids 12 (10) (2000) 2367 – 2371, doi:10.1063/1.1289396.

[18] V. S. Nikolayev, Oscillatory instability of the gas-liquid meniscus in a capillary under the imposed temperature difference, Int. J. Heat Mass Transfer 64 (2013) 313 – 321, doi:10.1016/j.ijheatmasstransfer.2013.04.043.